Kołowrocki Krzysztof, 0000-0002-4836-4976
Polish Safety and Reliability Association, Gdynia, Poland, ks.kolowrocki{at}gmail.com

Safety analysis of complex multistate ageing system

Keywords

multistate system, ageing, operation process impact, safety, transport, port oil terminal, maritime ferry

Abstract

Recent developments of an innovative own earlier approach to safety analysis of a complex multistate ageing system impacted by its operation processes are presented. A safety function and other safety indicators are defined for a complex multistate ageing system changing its functional structure and consequently its safety structure and its components safety parameters during the operation and determined under the assumption that its components have piecewise exponential safety functions. Results are applied to examine safety of port and maritime transportation systems.

1. Introduction

To perform the investigation of the complex multistate ageing technical system safety (Bautista et al., 2020; Brunelle & Kapur, 1999; Dąbrowska, 2020; Kołowrocki, 2000, 2003, 2005, 2008, 2011, 2014, 2020b, 2021b; Kołowrocki & Magryta-Mut, 2020; Kossow & Preuss, 1995; Kvassay et al., 2020; Li & Pham, 2005; Natvig, 2007; Szymkowiak, 2018a, 2018b, 2019; Wang et al., 2011, Xue, 1985, Xue & Yang, 1995a, 1995b; Yingkui & Jing, 2012; Zaitseva & Levashenko, 2017), the semi-Markov process model (Ferreira & Pacheco, 2007; Glynn & Haas, 2006; Grabski, 2014; Limnios & Oprisan, 2005; Mercier, 2008; Tang et al., 2007), can be used to describe this system operation process (Kołowrocki 2014; Magryta 2020). The system operation process model, under the assumption on the system safety multistate model (Xue & Yang, 1985; Xue, 1995), can be used to construct the general safety model of the complex multistate system changing its functional structure and its components safety parameters during variable operation conditions (Kołowrocki, 2014). Further, using this general model, it is possible to define the complex system main safety characteristics such as the system safety function, the mean values and standard deviations of the system lifetimes in the system safety state subsets and in the system particular safety states (Dąbrowska, 2020; Kołowrocki, 2014, 2020a, 2020b; Magryta, 2020). Other system safety indicators, like the system risk function, the system fragility curve, the moment when the system risk function exceeds a permitted level, the system intensity of ageing, the coefficient of operation process impact on system intensity of ageing and the system resilience indicator to operation process impact, can be introduced as well (Gouldby et al., 2010; Kołowrocki, 2014; Lauge et al., 2015; Szymkowiak, 2018a, 2018b, 2019).

The Chapter is organized into 5 parts, this Introduction as Section 1, Sections 2–4 and Conclusion as Section 5. In Section 2, the multistate approach to ageing system safety analysis is introduced. In Section 3, the safety model of the multistate ageing system impacted by its operation process is developed and its safety indicators are introduced. In Section 4, the applications of the developed model to safety examination of the port oil critical infrastructure (Kołowrocki, 2020a) and the maritime ferry technical system (Kołowrocki & Kuligowska, 2018) are presented. In Conclusion, the evaluation of results achieved is done and the per-

Safety and Reliability of Systems and Processes, Summer Safety and Reliability Seminar 2023.

DOI: 10.26408/srsp-2023-07.

spective for future research in the field of the complex technical systems including critical infrastructures safety (Ancione et al., 2020; Berg & Petrek, 2018; Bogalecka, 2020; Kołowrocki, 2022b; Kosmowski, 2021; Lauge et al., 2015; Magryta-Mut, 2023a) is proposed.

2. Multistate approach to ageing system safety analysis

2.1. System safety model

Similarly, as in the case of multistate approach to system reliability (Kołowrocki, 2014), in the multistate system safety analysis to define the system with degrading/ageing components, we assume that:

- n is the number of the system components (assets);
- E_i, $i = 1,2,\ldots,n$, are the system components,
- all components and the system have the safety state set $\{0,1,\ldots,z\}$, $z \geq 1$,
- the safety states are ordered, the safety state 0 is the worst and the safety state z is the best,
- $r, r \in \{1,2,\ldots,z\}$, is the critical safety state (the system and its components staying in the safety states less than the critical state, i.e. in safety states $0,1,2\ldots,r-1$, is highly dangerous for them and for their operating area),
- $T_i(u)$, $i = 1,2,\ldots,n$, are random variables representing the lifetimes of system components E_i in the safety state subset $\{u, u+1,\ldots,z\}$, $u = 0,1,2,\ldots,z$, while they were in the safety state z at the moment $t = 0$,
- $T(u)$ is a random variable representing the lifetime of the system in the safety state subset $\{u, u+1,\ldots,z\}$, $u = 0,1,2,\ldots,z$, while it was in the safety state z at the moment $t = 0$,
- the components and the system safety states degrade with time t,
- $s_i(t)$ is the component E_i, $i = 1,2,\ldots,n$, safety state at the moment $t, t \in \langle 0,\infty)$, while it was in the safety state z at the moment $t = 0$,
- $s(t)$ is the system safety state at the moment t, $t \in \langle 0,\infty)$, given that it was in the safety state z at the moment $t = 0$.

The above assumptions mean that the safety states of the system and its degrading components may be changed in time only from better safety states to worse safety states and not necessarily to the neighboring ones. This system ageing property is illustrated in Figure 1 and Figure 2.

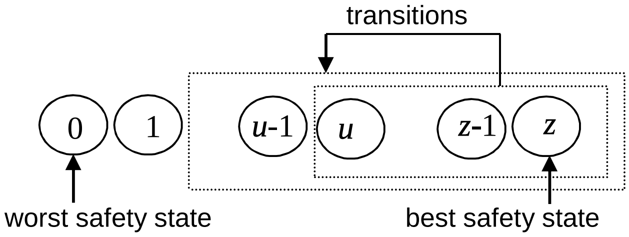

Figure 1. Illustration of system safety states changing

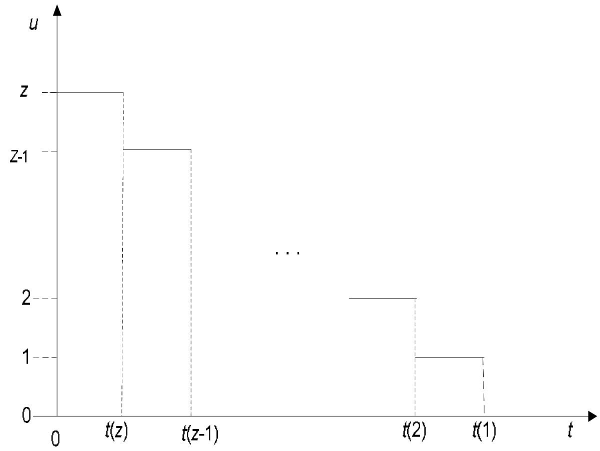

Figure 2. Relationship between realizations $t(u)$, $u = 1, 2,\ldots,z$, of system lifetime $T(u)$, $u = 1,2,\ldots,z$, in safety state subsets $\{u, u+1,\ldots,z\}$, $u = 1,2,\ldots,z$.

2.2. System safety indicators

We define the system safety function by the vector

$$\boldsymbol{S}(t,\cdot) = [\boldsymbol{S}(t,1), \boldsymbol{S}(t,2),\ldots,\boldsymbol{S}(t,z)], \quad (1)$$

for $t \in \langle 0,\infty)$, where the coordinate

$$\boldsymbol{S}(t,u) = P(s(t) \geq u \mid s(0) = z) = P(T(u) > t) \quad (2)$$

defined for $t \in \langle 0,\infty)$, $u = 1,2,\ldots,z$, is the probability that the multistate system is in the safety state subset $\{u, u+1,\ldots,z\}$, $u = 1,2,\ldots,z$, at the moment $t, t \in \langle 0,\infty)$, while it was in the safety state z at the moment $t = 0$.

We omit in the vector (1) the coordinate $\boldsymbol{S}(t,0)$ as

$$\boldsymbol{S}(t,0) = P(s(t) \geq 0 \mid s(0) = z) = P(T(0) > t) = 1$$

for $t \in \langle 0,\infty)$, what means that it is constant in time.

The coordinates $\boldsymbol{S}(t,u), t \in \langle 0,\infty), u = 1,2,\ldots,z$, defined by (2) are called the coordinate safety functions of the system safety function $\boldsymbol{S}(t,\cdot)$, $t \in \langle 0,\infty)$, defined by (1). Thus, the relationship between the distribution function $\boldsymbol{F}(t,u)$,

$t \in \langle 0,\infty), u = 1,2,\ldots,z$, of the system lifetime (u), $u = 1,2,\ldots,z$, in the safety state subset $\{u, u+1,\ldots,z\}$, $u = 1,2,\ldots,z$, and the coordinate safety function $\boldsymbol{S}(t,u)$, $t \in \langle 0,\infty)$, $u = 1,2,\ldots,z$, of its safety function $\boldsymbol{S}(t,\cdot)$, $t \in \langle 0,\infty)$, defined by (1), is given by

$$\boldsymbol{F}(t,u) = P(T(u) \le t) = 1 - P(T(u) > t)$$

$$= 1 - \boldsymbol{S}(t,u), t \in \langle 0,\infty), u = 1,2,\ldots,z. \qquad (3)$$

The exemplary graph of a four-state ($z = 3$) system safety function

$$\boldsymbol{S}(t,\cdot) = [\boldsymbol{S}(t,1), \boldsymbol{S}(t,2), \boldsymbol{S}(t,3)], t \in \langle 0,\infty),$$

is shown in Figure 3.

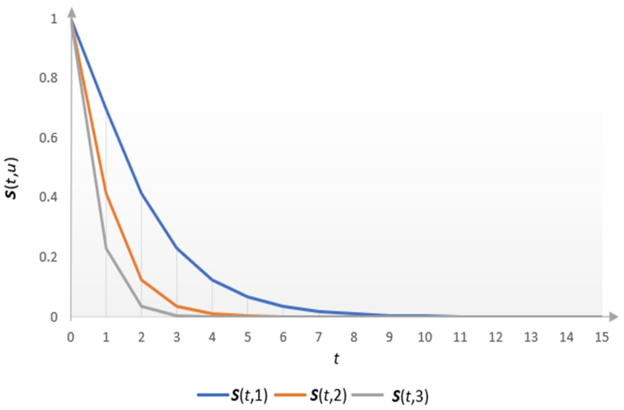

Figure 3. The graphs of a four-state system safety function $S(t,\cdot)$ coordinates.

If r is the critical safety state, then the multistate ageing system risk function

$$\boldsymbol{r}(t) = P(s(t) < r | s(0) = z) = P(T(r) \le t) \qquad (4)$$

defined for $t \in \langle 0,\infty)$ is the probability that the system at the moment $t, t \in \langle 0,\infty)$, is in the subset of safety states worse than the critical safety state $r, r \in \{1,2,\ldots,z\}$, while it was in the best safety state z at the moment $t = 0$ and by (3) and (4) it is given by

$$r(t) = 1 - \boldsymbol{S}(t,r), t \in \langle 0,\infty), \qquad (5)$$

where $\boldsymbol{S}(t,r)$ is the coordinate safety function of the multistate system safety function (1) defined by (2) for $u = r$.
The graph of the exemplary system risk function is presented in Figure 4.

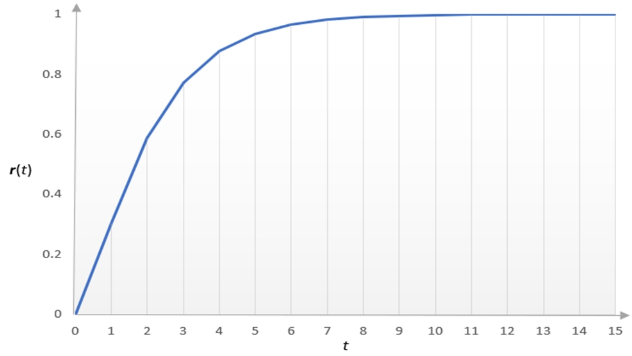

Figure 4. The graph of exemplary system risk function $r(t)$.

The moment t, when system risk function exceeds a permitted level d, $d \in (0,1)$, is defined by

$$t = \boldsymbol{r}^{-1}(\delta), \qquad (6)$$

where $\boldsymbol{r}^{-1}(t)$, $t \in \langle 0,\infty)$, is the inverse function of the risk function $\boldsymbol{r}(t)$, $t \in \langle 0,\infty)$, given by (5).
The intensities of ageing (degradation) of a multistate ageing system, i.e. the intensities of a system departure from safety state subsets $\{u, u+1,\ldots,z\}$, $u = 1,2,\ldots,z$, are defined by

$$\boldsymbol{\lambda}(t,u) = \frac{-\frac{d\boldsymbol{S}(t,u)}{dt}}{\boldsymbol{S}(t,u)}, t \in \langle 0,\infty), u = 1,2,\ldots,z, \qquad (7)$$

where (t,u), $u = 1,2,\ldots,z$, are the coordinate safety functions of the multistate ageing system safety function (1) defined by (2).
Hence, the multistate ageing system limit intensities of ageing can be found from the formulae

$$\boldsymbol{\lambda}(u) = \lim_{t\to\infty} \boldsymbol{\lambda}(t,u), u = 1,2,\ldots,z. \qquad (8)$$

Whereas, the multistate ageing system approximate mean intensities of ageing can be defined by

$$\boldsymbol{\lambda}(u) = \frac{1}{\boldsymbol{\mu}(u)}, u = 1,2,\ldots,z, \qquad (9)$$

where (u), $u = 1,2,\ldots,z$, are the mean values of the multistate ageing system lifetimes in the safety state subsets $\{u, u+1,\ldots,z\}$, $u = 1,2,\ldots,z$, given by

$$\boldsymbol{\mu}(u) = \int_0^\infty \boldsymbol{S}(t,u)dt, u = 1,2,\ldots,z, \qquad (10)$$

and $\boldsymbol{S}(t,u)$, $u = 1,2,\ldots,z$, $b = 1,2,\ldots,v$ are coordinate safety functions defined by (2).

The coefficients of the outside impact on the multistate ageing system safety are defined by

$$\boldsymbol{\rho}(t,u) = \boldsymbol{\lambda}(t,u)/\boldsymbol{\lambda}^0(t,u), \quad (11)$$

$t \in \langle 0,\infty), u = 1,2,\dots,z,$

or by

$$\boldsymbol{\rho}(u) = \boldsymbol{\lambda}(u)/\boldsymbol{\lambda}^0(u), u = 1,2,\dots,z, \quad (12)$$

where $\boldsymbol{\lambda}(t,u)$, $\boldsymbol{\lambda}(u)$ and $\boldsymbol{\lambda}^0(t,u)$, $\boldsymbol{\lambda}^0(u)$, $u = 1,2,\dots,z$, respectively are, the intensities of ageing of the multistate ageing system with and without outside impact, determined respectively according to (7), (8) and (9).

Finally, we define the multistate ageing system resilence indicators, i.e. the coefficients of the multistate ageing system resilience to the outside impact, by

$$\boldsymbol{RI}(t,u) = \frac{1}{\boldsymbol{\rho}(t,u)}, t \in \langle 0,\infty), u = 1,2,\dots,z, \quad (13)$$

or by

$$\boldsymbol{RI}(u) = \frac{1}{\boldsymbol{\rho}(u)}, u = 1,2,\dots,z, \quad (14)$$

where $\boldsymbol{\rho}(t,u)$ and $\boldsymbol{\rho}(u)$, $u = 1,2,\dots,z$, are the coefficients of the outside impact on the multistate ageing system safety, respectively defined by (11) and (12).

2.3. System safety structures

On the basis of the multistate approach to ageing system safety analysis proposed in Section 2.1, considering definition of safety function introduced in Section 2.2, we may define basic multistate ageing system safety structures.

Definition 1

A multistate ageing system composed of n assets A_i, $i = 1,2,\dots,n$, is called series if its lifetime $T(u)$, $u = 1,2,\dots,z$, in the safety state subset $\{u,u+1,\dots,z\}$, $u = 1,2,\dots,z$, is given by

$$T(u) = \min_{1\le i\le n}\{T_i(u)\}, u = 1,2,\dots,z,$$

where $T_i(u)$, $u = 1,2,\dots,z$, $i = 1,2,\dots,n$ are the lifetimes of the assets A_i, $i = 1,2,\dots,n$, in the safety state subset $\{u,u+1,\dots,z\}$, $u = 1,2,\dots,z$. The number n is called the system safety structure shape parameter. considering definition of safety function introduced in Section 2.2, we may define basic multistate ageing system safety structures.

Definition 2

A multistate ageing system composed of n assets A_i, $i = 1,2,\dots,n$, is called series if its lifetime $T(u)$, $u = 1,2,\dots,z$, in the safety state subset $\{u,u+1,\dots,z\}$, $u = 1,2,\dots,z$, is given by

$$T(u) = \min_{1\le i\le n}\{T_i(u)\}, u = 1,2,\dots,z,$$

where $T_i(u)$, $u = 1,2,\dots,z$, $i = 1,2,\dots,n$ are the lifetimes of the assets A_i, $i = 1,2,\dots,n$, in the safety state subset $\{u,u+1,\dots,z\}$, $u = 1,2,\dots,z$. The number n is called the system safety structure shape parameter.

The above definition means that the series multistate ageing system is in the safety state subset $\{u,u+1,\dots,z\}$, $u = 1,2,\dots,z$, if and only if all its n assets are in this subset of safety states. That meaning is very close to the definition of a two-state system considered in a classical reliability analysis that is not failed if all its all assets are not failed (Kołowrocki, 2014). This fact can justify the safety structure scheme for a series multistate ageing system presented in Figure 5.

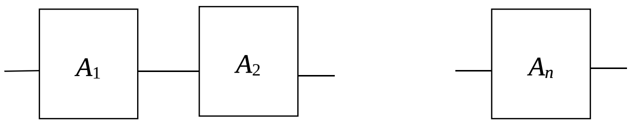

Figure 5. The scheme of a series multistate ageing system safety structure.

It is easy to work out that the safety function of the series multistate ageing system, is given by the vector (Kołowrocki, 2014)

$$\boldsymbol{S}(t,\cdot) = [\boldsymbol{S}(t,1),\boldsymbol{S}(t,2),...,\boldsymbol{S}(t,z)],\ t \in \langle 0,\infty),$$

with the coordinate safety functions

$$S(t,u) = \prod_{i=1}^{n} S_i(t,u)\,, t \in \langle 0,\infty), u = 1,2,\dots,z.$$

Definition 3

A multistate ageing system composed of n assets A_i, $i = 1,2,\dots,n$, is called parallel if its lifetime

$T(u)$, $u = 1,2,\dots,z$, in the safety state subset $\{u, u+1,\dots,z\}$, $u = 1,2,\dots,z$, is given by

$$T(u) = \max_{1\le i\le n}\{T_i(u)\},\ u = 1,2,\dots,z,$$

where $T_i(u)$, $u = 1,2,\dots,z$, $i = 1,2,\dots,n$ are the lifetimes of the assets A_i, $i = 1,2,\dots,n$, in the safety state subset $\{u, u+1,\dots,z\}$, $u = 1,2,\dots,z$.

The number n is called the system structure safety shape parameter.

The above definition means that the parallel multistate ageing system is in the safety state subset $\{u, u+1,\dots,z\}$, $u = 1,2,\dots,z$, if and only if at least one of its n assets is in this subset of safety states. That meaning is very close to the definition of a two-state parallel system in a classical reliability analysis that is not failed if at least one of its components is not failed what can justify the parallel multistate ageing system safety structure scheme presented in Figure 6.

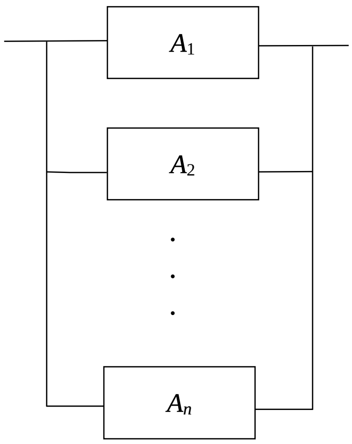

Figure 6. The scheme of a parallel multistate ageing system safety structure.

The safety function of the parallel multistate ageing system is given by the vector (Kołowocki, 2014)

$$\boldsymbol{S}(t,\cdot) = [\boldsymbol{S}(t,1),\boldsymbol{S}(t,2),\dots,\boldsymbol{S}(t,z)],\ t \in \langle 0,\infty)$$

with the coordinate safety functions

$$S(t,u) = 1 - \prod_{i=1}^{n}[1 - S_i(t,u)],$$

$t \in \langle 0,\infty)$, $u = 1,2,\dots,z$.

Definition 4

A multistate ageing system composed of n assets A_i, $i = 1,2,\dots,n$, is called an „*m* out of *n*" if its lifetime $T(u)$, $u = 1,2,\dots,z$, in the safety state subset $\{u, u+1,\dots,z\}$, $u = 1,2,\dots,z$, is given by

$$T(u) = T_{(n-m+1)}(u)\ m = 1,2,\dots,n,\ u = 1,2,\dots,z,$$

where $T_{(n-m+1)}(u)$, $m = 1,2,\dots,n$, $u = 1,2,\dots,z$, is the (n-m+1)-th order statistic in the sequence of the asset lifetimes

$$T_1(u), T_2(u),\dots,T_n(u),\ u = 1,2,\dots,z.$$

The above definition means that the „*m* out of *n*" multistate ageing system is in the safety state subset $\{u, u+1,\dots,z\}$, $u = 1,2,\dots,z$, if and only if at least m out of its n assets are in this safety state subset and it is a parallel system if $m = 1$ and it is a series system if $m = n$. The numbers m and n are called the system safety structure shape parameters. The scheme of an „*m* out of *n*" multistate ageing system safety structure, justified in an analogous way as in the cases of series and parallel multistate ageing systems, is given in Figure 7, where $i_1, i_2, \dots, i_n \in \{1,2,\dots n\}$ and $i_a \ne i_b$ for $a \ne b$.

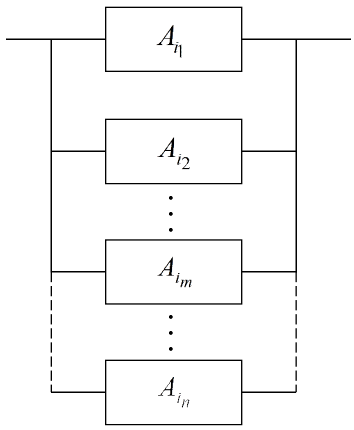

Figure 7. The scheme of an „*m* out of *n*" multistate ageing system safety structure.

It can be simply shown that the safety function of the „*m* out of *n*" multistate ageing system is given by the vector (Kolowrocki, 2014)

$$\boldsymbol{S}(t,\cdot) = [\boldsymbol{S}(t,1),\boldsymbol{S}(t,2),\dots,\boldsymbol{S}(t,z)],\ t \in \langle 0,\infty),$$

with the coordinate safety functions

$$S(t,u) = \sum_{\substack{r_1,r_2,\dots,r_n \in \{0,1\} \\ m \le r_1+r_2+\dots+r_n \le n}} [S_i(t,u)]^{r_i} \cdot$$

$$\cdot [1 - S_i(t,u)]^{1-r_i},\ t \in \langle 0,\infty),\ u = 1,2,\dots,z,$$

or equivalently with the coordinate safety functions

$$S(t,u) = \sum_{\substack{r_1,r_2,\dots,r_n \in \{0,1\} \\ 0 \le r_1+r_2+\dots+r_n \le m-1}} [S_i(t,u)]^{r_i} \cdot$$

$$\cdot [1 - S_i(t,u)]^{1-r_i},\ t \in \langle 0,\infty),\ u = 1,2,\dots,z,$$

Definitions of other multistate ageing system safety structures can be found in (Kołowrocki, 2014).

3. Safety of multistate ageing system impacted by its operation process

3.1. Semi-Markov model of system operation process

We assume that the system during its operation process is taking ν, $\nu \in N$, different operation states $z_1, z_2, \dots, z_\nu$. Further, we define the system operation process $Z(t)$, $t \in \langle 0,\infty)$, with discrete operation states from the set $\{z_1, z_2, \dots, z_\nu\}$.
Moreover, we assume that the system operation process $Z(t)$ is a semi-Markov process (Ferreira & Pacheco, 2007; Glynn & Haas, 2006; Grabski, 2014; Limnios & Oprisan, 2005; Mercier, 2008; Tang et al., 2007) with the conditional sojourn times θ_{bl} at the operation states z_b when its next operation state is z_l, $b,l = 1,2,\dots,\nu$, $b \neq l$. Under these assumptions, the system operation process may be described by the following parameters (Kołowrocki, 2014):

- the vector $[p_b(0)]_{1x\nu}$ of the initial probabilities

$$p_b(0) = P(Z(0) = z_b),\ b = 1,2,\dots,\nu, \quad (15)$$

  of the system operation process $Z(t)$ staying at particular operation states at the moment $t = 0$,
- the matrix $[p_{bl}]_{\nu x\nu}$ of probabilities

$$p_{bl},\ b,l = 1,2,\dots,\nu,\ b \neq l, \quad (16)$$

  of the system operation process $Z(t)$ transitions between the operation states z_b and z_l,
- the matrix $[H_{bl}(t)]_{\nu x\nu}$ of conditional distribution functions

$$H_{bl}(t) = P(\theta_{bl} < t), \quad (17)$$

$$t \in \langle 0,\infty),\ b,l = 1,2,\dots,\nu,\ b \neq l,$$

  of the system operation process $Z(t)$ conditional sojourn times θ_{bl} at the operation states or equivalently by the matrix $[h_{bl}(t)]_{\nu x\nu}$ of the conditional density functions

$$h_{bl}(t) = \frac{dH_{bl}(t)}{dt} \quad (18)$$

$$t \in \langle 0,\infty),\ b,l = 1,2,\dots,\nu,\ b \neq l,$$

  of the system operation process $Z(t)$ conditional sojourn times θ_{bl} at the operation states corresponding to the conditional distribution functions $H_{bl}(t)$.

The knowledge of the system operation process parameters gives the possibility of finding its main characteristics:

- the mean values M_b, $b = 1,2,\dots,\nu$, of the system operation process $Z(t)$ unconditional sojourn times θ_b, $b = 1,2,\dots,\nu$, at the operation states z_b, $b = 1,2,\dots,\nu$,

$$M_b = \sum_{l=1}^{\nu} p_{bl} M_{bl},\ b = 1,2,\dots,\nu, \quad (19)$$

  where

$$M_{bl} = \int_0^\infty dH_{bl}(t) = \int_0^\infty t h_{bl}(t)dt, \quad (20)$$

  for $b,l = 1,2,\dots,\nu$, $b \neq l$,

  are the mean values of the conditional sojourn times θ_{bl} at the operation states z_b when its next operation state is z_l, $b,l = 1,2,\dots,\nu$, $b \neq l$,
- the limit values

$$p_b = \lim_{t\to\infty} p_b(t)$$

  of the system operation process $Z(t)$ transient probabilities at the particular operation states

$$p_b(t) = P(Z(t) = z_b),$$

$t \in \langle 0, \infty), b = 1,2,\dots,\nu,$

given by

$$p_b = \frac{\pi_b M_b}{\sum_{l=1}^{\nu} \pi_l M_l}, b = 1,2,\dots,\nu, \quad (21)$$

where π_b, $b = 1,2,\dots,\nu$, are the steady probabilities of the vector $[\pi_b]_{1x\nu}$, satisfying the system of equations

$$\begin{cases}[\pi_b] = [\pi_b][p_{bl}] \\ \sum_{l=1}^{\nu} \pi_l = 1,\end{cases} \quad (22)$$

- the approximate mean values $\widehat{M}_b$, $b = 1,2,\dots,\nu$, of the system operation process $Z(t)$ total sojourn times $\hat{\theta}_b$ at the particular operation states z_b, $b = 1,2,\dots,\nu$, during the large fixed system opetation time θ, given by

$$\widehat{M}_b \cong p_b \theta, b = 1,2,\dots,\nu. \quad (23)$$

3.2. Safety of system related to its operation process

We assume that the changes of the operation states of the system operation process $Z(t)$ have an influence on the safety of system components E_i, $i = 1,2,\dots,n$, and on the system functional structure and consequently on the system safety structure as well. Thus, we denote the system multistate component E_i, $i = 1,2,\dots,n$, conditional lifetime in the safety state subset $\{u, u+1,\dots,z\}$, $u = 1,2,\dots,z$, while the system is at the operation state z_b, $b = 1,2,\dots,\nu$, by $[T_i(u)]^{(b)}$, $u = 1,2,\dots,z$, $b = 1,2,\dots,\nu$, $i = 1,2,\dots,n$, and its conditional safety function by the vector

$$[S_i(t,\cdot)]^{(b)} = [[S_i(t, 1)]^{(b)},\dots,[S_i(t,z)]^{(b)}], \quad (24)$$

$t \in \langle 0, \infty), u = 1,2,\dots,z,$

$b = 1,2,\dots,\nu, i = 1,2,\dots,n,$

with the coordinates defined by

$$[S_i(t,u)]^{(b)} = P([T_i(u)]^{(b)} > t | Z(t) = z_b), \quad (25)$$

$t \in \langle 0, \infty), u = 1,2,\dots,z,$

$b = 1,2,\dots,\nu, i = 1,2,\dots,n.$

The coordinate safety function $[S_i(t,u)]^{(b)}$, $u = 1,2,\dots,z$, $b = 1,2,\dots,\nu$, $i = 1,2,\dots,n$, is the conditional probability that the system component E_i, $i = 1,2,\dots,n$, lifetime $[T_i(u)]^{(b)}$, $u = 1,2,\dots,z$, $b = 1,2,\dots,\nu$, $i = 1,2,\dots,n$, in the safety state subset $\{u, u+1,\dots,z\}$, $u = 1,2,\dots,z$, is greater than $t, t \in \langle 0, \infty)$, while the system operation process $Z(t)$, $t \in \langle 0, \infty)$, is at the operation state z_b, $b = 1,2,\dots,\nu$.
Similarly, we denote the system conditional lifetime in the safety state subset $\{u, u+1,\dots,z\}$, $u = 1,2,\dots,z$, while the system is at the operation state z_b, $b = 1,2,\dots,\nu$, by $[T(u)]^{(b)}$, $u = 1,2,\dots,z$, $b = 1,2,\dots,\nu$, and the conditional safety function of the system by the vector

$$[S(t,\cdot)]^{(b)} = [[S(t,1)]^{(b)},\dots,[S(t,z)]^{(b)}], \quad (26)$$

$t \in \langle 0, \infty), b = 1,2,\dots,\nu,$

with the coordinates defined by

$$[\boldsymbol{S}(t,u)]^{(b)} = P([T(u)]^{(b)} > t | Z(t) = z_b), \quad (27)$$

$t \in \langle 0, \infty), u = 1,2,\dots,z, b = 1,2,\dots,\nu.$

The conditional coordinate safety function $[\boldsymbol{S}(t,u)]^{(b)}$, $t \in \langle 0, \infty)$, $u = 1,2,\dots,z$, $b = 1,2,\dots,\nu$, defined by (27), is the conditional probability that the system lifetime $[T(u)]^{(b)}$, $u = 1,2,\dots,z$, $b = 1,2,\dots,\nu$, in the safety state subset $\{u, u+1,\dots,z\}$, $u = 1,2,\dots,z$, is greater than $t, t \in \langle 0, \infty)$, while the system operation process $Z(t)$, $t \in \langle 0, \infty)$, is at the operation state z_b, $b = 1,2,\dots,\nu$.
Thus, the system conditional lifetimes in the safety states subset $\{u, u+1,\dots,z\}$, $u = 1,2,\dots,z$, at the operation state z_b, $b = 1,2,\dots,\nu$,

$$[T(u)]^{(b)}$$

$$= T([T_1(u)]^{(b)}, [T_2(u)]^{(b)},\dots,[T_n(u)]^{(b)}),$$

defined for $u = 1,2,\dots,z$, $b = 1,2,\dots,\nu$, $n \in N$, are dependent on the components conditional lifetimes $[T_1(u)]^{(b)}, [T_2(u)]^{(b)},\dots,[T_n(u)]^{(b)}$, in the safety states subset $\{u, u+1,\dots,z\}$, $u = 1,2,\dots,z$, at the operation state z_b,

$b = 1,2,\ldots,\nu$, and the coordinates of the system conditional safety function at the operation state z_b, $b = 1,2,\ldots,\nu$,

$$[\boldsymbol{S}(t,u)]^{(b)}$$

$$= \boldsymbol{S}([S_1(t,u)]^{(b)}, [S_2(t,u)]^{(b)}, \ldots, [S_n(t,u)]^{(b)})$$

defined for $t \in \langle 0,\infty)$, $u = 1,2,\ldots,z$, $b = 1,2,\ldots,\nu$, $n \in N$, are dependent on the coordinate safety functions

$$[S_1(t,u)]^{(b)}, [S_2(t,u)]^{(b)}, \ldots, [S_n(t,u)]^{(b)},$$

$$t \in \langle 0,\infty), u = 1,2,\ldots,z, b = 1,2,\ldots,\nu,$$

of the components conditional coordinate safety functions at the operation state z_b, $b = 1,2,\ldots,\nu$, defined by (25).

Further, we assume that the system components E_i, $i = 1,2,\ldots,n$, at the system operation states z_b, $b = 1,2,\ldots,\nu$, have piecewise exponential safety functions, i.e. their coordinate safety functions are given by

$$[S_i(t,u)]^{(b)} = P([T_i(u)]^{(b)} > t | Z(t) = z_b)$$

$$= \exp[-[\lambda_i(u)]^{(b)} t], t \in \langle 0,\infty), \quad (28)$$

$$u = 1,2,\ldots,z, b = 1,2,\ldots,\nu, i = 1,2,\ldots,n,$$

and we conclude that the system conditional coordinate safety functions are dependent of these piecewise exponential safety functions.

Consequently, we denote the system unconditional lifetime in the safety state subset $\{u, u+1,\ldots,z\}$, $u = 1,2,\ldots,z$, by $T(u)$, $u = 1,2,\ldots,z$, and the unconditional safety function of the system by the vector

$$\boldsymbol{S}(t,\cdot) = [\boldsymbol{S}(t,1),\ldots,\boldsymbol{S}(t,z)], t \in \langle 0,\infty), \quad (29)$$

with the coordinate safety functions defined by

$$\boldsymbol{S}(t,u) = P(T(u) > t), \quad (30)$$

$$t \in \langle 0,\infty), u = 1,2,\ldots,z.$$

In the case when the system operation time θ is large enough and the condition (28) is fulfilled, the coordinate safety functions of the unconditional safety function (30) of the system defined by (29) are given by

$$\boldsymbol{S}(t,u) \cong \sum_{b=1}^{\nu} p_b [\boldsymbol{S}(t,u)]^{(b)}, \quad (31)$$

$$t \in \langle 0,\infty), u = 1,2,\ldots,z,$$

where $[\boldsymbol{S}(t,u)]^{(b)}$, $t \in \langle 0,\infty)$, $u = 1,2,\ldots,z$, $b = 1,2,\ldots,\nu$, are the conditional coordinate safety functions of the system conditional safety functions defined by (26)–(27) and p_b, $b = 1,2,\ldots,\nu$, are the system operation process limit transient probabilities determined by (21).

Hence, the mean value of the system unconditional lifetime $T(u)$, $u = 1,2,\ldots,z$, in the safety state subset $\{u, u+1,\ldots,z\}$, $u = 1,2,\ldots,z$, is given by (Kołowrocki, 2014)

$$\boldsymbol{\mu}(u) \cong \sum_{b=1}^{\nu} p_b [\boldsymbol{\mu}(u)]^{(b)}, u = 1,2,\ldots,z, \quad (32)$$

where $[\boldsymbol{\mu}(u)]^{(b)}$, $u = 1,2,\ldots,z$, $b = 1,2,\ldots,\nu$, are the mean values of the system conditional lifetimes $[T(u)]^{(b)}$, $u = 1,2,\ldots,z$, $b = 1,2,\ldots,\nu$, in the safety state subset $\{\{u, u+1,\ldots,z\}$, $u = 1,2,\ldots,z$, at the operation state z_b, $b = 1,2,\ldots,\nu$, given by

$$[\boldsymbol{\mu}(u)]^{(b)} = \int_0^\infty [\boldsymbol{S}(t,u)]^{(b)} dt, \quad (33)$$

$$u = 1,2,\ldots,z, b = 1,2,\ldots,\nu,$$

where $[\boldsymbol{S}(t,u)]^{(b)}$, $t \in \langle 0,\infty)$, $u = 1,2,\ldots,z$, $b = 1,2,\ldots,\nu$, are defined by (26)–(27) and p_b, $b = 1,2,\ldots,\nu$, are determined by (21).

Whereas, the variance of the system unconditional lifetime $T(u)$ is given by

$$\boldsymbol{\sigma}^2(u) \cong 2\int_0^\infty t\, \boldsymbol{S}(t,u) dt - [\boldsymbol{\mu}(u)]^2, \quad (34)$$

$$u = 1,2,\ldots,z,$$

where $\boldsymbol{S}(t,u)$, $t \in \langle 0,\infty)$, $u = 1,2,\ldots,z$, are given by (31) and $\boldsymbol{\mu}(u)$, $u = 0,1,\ldots,z$, are given by (32).

Further, we get the following formulae for the mean values of the unconditional lifetimes of the system in particular safety states

$$\bar{\boldsymbol{\mu}}(u) \cong \boldsymbol{\mu}(u) - \boldsymbol{\mu}(u+1), u = 1,2,\ldots,z-1,$$

$$\bar{\boldsymbol{\mu}}(z) \cong \boldsymbol{\mu}(z), \tag{35}$$

where $\mu(u)$, $u = 0,1,\dots,z$, are determined by (32).
Moreover, if r is the system critical safety state, then the system risk function is given by

$$r(t) \cong 1 - \boldsymbol{S}(t,r),\ t \in \langle 0,\infty), \tag{36}$$

where $\boldsymbol{S}(t,r)$, $t \in \langle 0,\infty)$, is the coordinate safety function of the system unconditional safety function (29) defined by (30) and given by (31) for $u = r$.
Next, if t is the moment when the system risk function exceeds a permitted level d, then

$$t \cong \boldsymbol{r}^{-1}(\delta), \tag{37}$$

where $\boldsymbol{r}^{-1}(t)$ is the inverse function of the risk function $\boldsymbol{r}(t)$ given by (36).
The intensities of ageing (degradation) of the system impacted by its operation process, i.e. the intensities of the system impacted by its operation process departure from the safety state subset $\{u, u+1,\dots,z\}$, $u = 1,2,\dots,z$, are given by

$$\boldsymbol{\lambda}(t,u) \cong \frac{-\frac{d\boldsymbol{S}(t,u)}{dt}}{\boldsymbol{S}(t,u)},\ t \in \langle 0,\infty),\ u = 1,2,\dots,z, \tag{38}$$

where $\boldsymbol{S}(t,u)$, $t \in \langle 0,\infty)$, $u = 1,2,\dots,z$, are determined by (31).
The multistate ageing system impacted by its operation process limit intensities of ageing can be found from the formulae

$$\boldsymbol{\lambda}(u) \cong \lim_{t\to\infty} \boldsymbol{\lambda}(t,u),\ u = 1,2,\dots,z, \tag{39}$$

where $\boldsymbol{\lambda}(t,u)$, $t \in \langle 0,\infty)$, $u = 1,2,\dots,z$, are given by (38).
Whereas, the multistate ageing system impacted by its operation process mean intensities of ageing can be found from

$$\boldsymbol{\lambda}(u) \cong \frac{1}{\boldsymbol{\mu}(u)},\ u = 1,2,\dots,z, \tag{40}$$

where (u), $u = 1,2,\dots,z$, are the mean values of the multistate ageing system impacted by its operation process lifetimes in the safety state subsets $\{u, u+1,\dots,z\}$, $u = 1,2,\dots,z$, given by (32).
Finally, we can determine the system resilience indicators:

- the coefficients of operation process impact on the system intensities of degradation, i.e. the system intensities of departure from the safety state subsets $\{u, u+1,\dots,z\}$, $u = 1,2,\dots,z$,

$$\boldsymbol{\rho}(t,u) \cong \frac{\boldsymbol{\lambda}(t,u)}{\boldsymbol{\lambda}^0(t,u)}, \tag{41}$$

$t \in \langle 0,\infty)$, $u = 1,2,\dots,z$,

and

$$\boldsymbol{\rho}(u) \cong \frac{\boldsymbol{\lambda}(u)}{\boldsymbol{\lambda}^0(u)},\ u = 1,2,\dots,z, \tag{42}$$

where $\boldsymbol{\lambda}^0(t,u)$, $t \in \langle 0,\infty)$ and $\boldsymbol{\lambda}^0(u)$, $u = 1,2,\dots,z$, are the intensities of degradation of the system without of operation process impact, whereas $\boldsymbol{\lambda}(t,u)$, $t \in \langle 0,\infty)$ and $\boldsymbol{\lambda}(u)$, $u = 1,2,\dots,z$, are the intensity of degradation of the system with the operation process impact given respectively by (38), (39) and (40),

- the indicators of system resilience to operation process impact defined by

$$\boldsymbol{RI}(t,u) \cong \frac{1}{\boldsymbol{\rho}(t,u)}, \tag{43}$$

$t \in \langle 0,\infty)$, $u = 1,2,\dots,z$,

or by

$$\boldsymbol{RI}(u) \cong \frac{1}{\boldsymbol{\rho}(u)},\ u = 1,2,\dots,z, \tag{44}$$

where $\boldsymbol{\rho}(t,u)$, $t \in \langle 0,\infty)$ and $\boldsymbol{\rho}(u)$, $u = 1,2,\dots,z$, are the coefficient of operation process impact on the system intensities of degradation given respectively by (41) and (42).

4. Application

4.1. Safety of port oil terminal critical infrastructure impacted by its operation process

We consider the port oil terminal critical infrastructure impacted by its operation process operating at the Baltic seaside that is designated for receiving oil products from ships, storage and sending them by carriages or trucks.
The port oil terminal critical infrastructure is com-

posed of three parts *A*, *B* and *C*, linked by the piping transportation system with the pier of Gdynia Port. The port oil terminal operating area is presented in Figures 8.
The main technical assets components (assets) of the port oil terminal critical infrastructure are:

- A_1 – port oil piping transportation system,
- A_2 – internal pipeline technological system,
- A_3 – supporting pump station,
- A_4 – internal pump system,
- A_5 – port oil tanker shipment terminal,
- A_6 – loading railway carriage station,
- A_7 – loading road carriage station,
- A_8 – unloading railway carriage station,
- A_9 – oil storage reservoir system.

Figure 8. The port oil terminal critical infrastructure operating area.

The port oil piping transportation system, the asset A_1, location in the Port of Gdynia is presented in Figure 9.

Figure 9. The port oil piping transportation system location in the Port of Gdynia.

The considered port oil piping transportation system, the asset A_1, functional structure is presented in Figure 10.

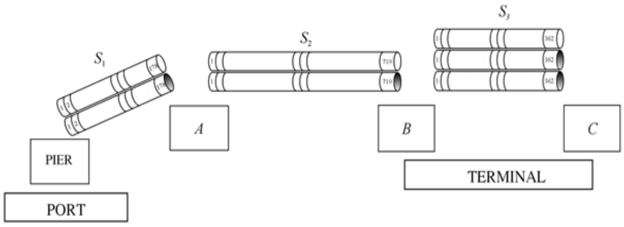

Figure 10. The port oil piping transportation system functional structure.

The port oil pipeline system safety structure presented in Figure 11.

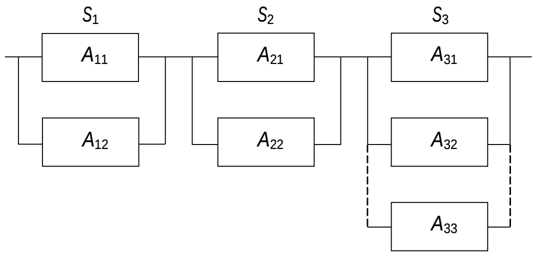

Figure 11. The scheme of the port oil piping transportation system safety structure.

The asset A_1, is a system composed of a series-parallel subsystems S_1, containing two pipelines (the assets A_1 and A_{12} with series safety structures), a series-parallel subsystems S_2, containing two pipelines (the assets A_{21} and A_{22} with series safety structures), and one „2 out of 3" subsystem S_3 containing 3 pipelines (the assets A_{31}, A_{32} and $A_{33}$with series safety structures). The subsystems S_1, S_2 and S_3 are forming a general series port oil pipeline system safety structure.
The asset A_1 operation is the main activity of the port oil terminal critical infrastructure involving its remaining assets $A_2 – A_9$ and determining their operation processes.
On the basis of the statistical data and expert opinions, it is possible to fix and to evaluate the following unknown basic parameters of the oil terminal critical infrastructure operation process:

- the number of operation process states v = 7, and the operation process states:
  - the operation state z_1, transport of one kind of medium from the terminal part *B* to part *C* using two out of three pipelines of the subsystem S_3 of the asset A_1 illustrated in Figure 12 and assets A_2, A_4, A_6, A_7, A_9,

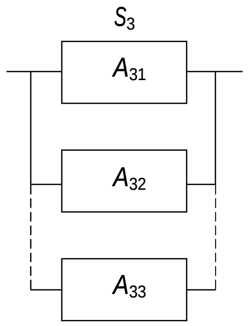

Figure 12. The scheme of the port oil piping transportation system safety structure at the operation state z_1.

– the operation state z_2, transport of one kind of medium from the terminal part *C* to part *B* using one out of three pipelines of the subsystem S_3 of the asset A_1 illustrated in Figure 13 and assets A_2, A_4, A_8, A_9,

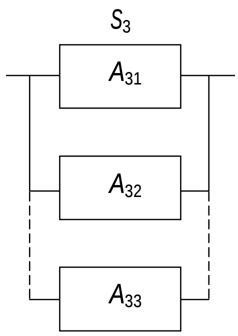

Figure 13. The scheme of the port oil piping transportation system safety structure at the operation state z_2.

– the operation state z_3, transport of one kind of medium from the terminal part *B* through part *A* to pier using one out of two pipelines of the subsystem S_1 and one out of two pipelines of the subsystem S_2 of the asset A_1 illustrated in Figure 14 and assets A_2, A_4, A_5, A_9,

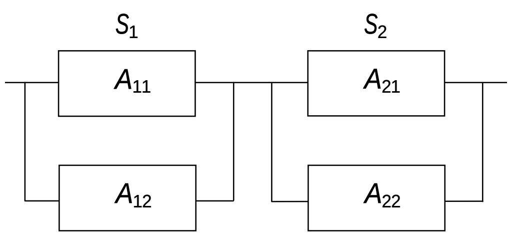

Figure 14. The scheme of the port oil piping transportation system safety structure at the operation state z_3.

– the operation state z_4, transport of one kind of medium from the pier through parts *A* and *B* to part *C* using one out of two pipelines of the subsystem S_1, one out of two pipelines in subsystem S_2 and two out of three pipelines of the subsystem S_3 of the asset A_1 illustrated in Figure 15 and assets A_2, A_3, A_4, A_5, A_6, A_7, A_9,

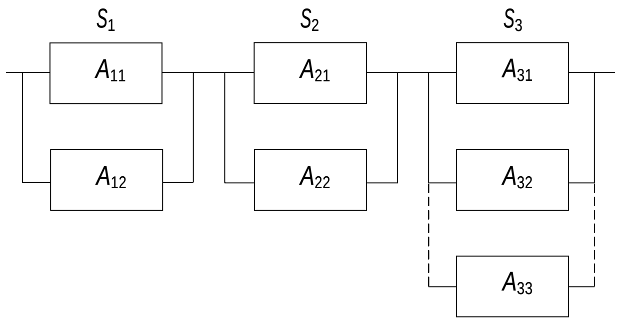

Figure 15. The scheme of the port oil piping transportation system safety structure at the operation state z_4.

– the operation state z_5, transport of one kind of medium from the pier through part *A* to *B* using one out of two pipelines of the subsystem S_1 and one out of two pipelines of the subsystem S_2 of the asset A_1 illustrated in Figure 16 and assets A_2, A_3, A_4, A_5, A_9,

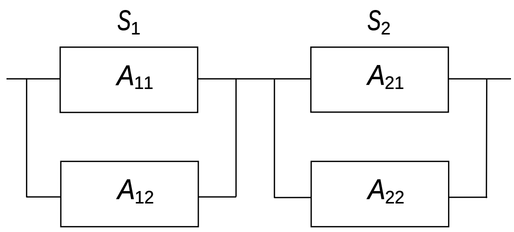

Figure 16. The scheme of the port oil piping transportation system safety structure at the operation state z_5.

– the operation state z_6, transport of one kind of medium from the terminal part *B* to *C* using two out of three pipelines of the subsystem S_3, and simultaneously transport one kind of medium from the pier through part *A* to *B* using one out of two pipelines of the subsystem S_1 and one out of two pipelines of the subsystem S_2 of the asset A_1 illustrated in Figure 17 and assets A_2, A_3, A_4, A_5, A_6, A_7, A_9,

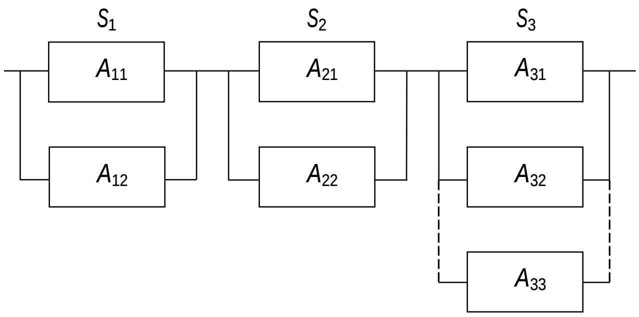

Figure 17. The scheme of the port oil piping transportation system safety structure at the operation state z_6.

– the operation state z_7, transport of one kind of medium from the terminal part *B* to *C* using one out of three pipelines of the subsystem S_3, and simultaneously transport second kind of medium from the terminal part *C* to *B* using one out of three pipelines of the subsystem S_3 of the asset A_1 illustrated in Figure 18 and assets A_2, A_4, A_6, A_7, A_8, A_9.

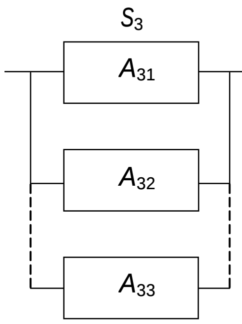

Figure 18. The scheme of the port oil piping transportation system safety structure at the operation state z_7.

To identify the unknown parameters of the port oil piping transportation system operation process the suitable statistical data coming from its real realizations should be collected on the basic of this data it is possible to estimate these parameters and to fix the port oil terminal characteristics. The port oil terminal critical infrastructure operation process $Z(t)$ main characteristics, the limit values of transient probabilities at the particular operation states z_b, $b = 1,2,\ldots,7$, are (Kołowrocki, 2020a):

$$p_1 = 0.395,\ p_2 = 0.060,\ p_3 = 0.003,\ p_4 = 0.002,\ p_5 = 0.200,\ p_6 = 0.058,\ p_7 = 0.282. \quad (45)$$

We distinguish the following three safety states ($z = 2$) of the system and its components:

- a safety state 2 – the components and the port oil terminal are fully safe,
- a safety state 1 – the components and the port oil terminal are less safe and more dangerous because of the possibility of environment pollution,
- a safety state 0 – the components and the port oil terminal are destroyed.

The port oil terminal system safety function is given by the vector

$$\boldsymbol{S}(t,\cdot) = [\boldsymbol{S}(t,1),\boldsymbol{S}(t,2)],\ t \in \langle 0,\infty), \quad (46)$$

with determined according to (31) and (45) the coordinate safety functions:

$$\boldsymbol{S}(t,1) = 0.395\cdot[\boldsymbol{S}(t,1)]^{(1)} + 0.060\cdot[\boldsymbol{S}(t,1)]^{(2)} + 0.003\cdot[\boldsymbol{S}(t,1)]^{(3)} + 0.002\cdot[\boldsymbol{S}(t,1)]^{(4)} + 0.2\cdot[\boldsymbol{S}(t,1)]^{(5)} + 0.058\cdot[\boldsymbol{S}(t,1)]^{(6)} + 0.282\cdot[\boldsymbol{S}(t,1)]^{(7)},\ t \in \langle 0,\infty), \quad (47)$$

$$\boldsymbol{S}(t,2) = 0.395\cdot[\boldsymbol{S}(t,2)]^{(1)} + 0.060\cdot[\boldsymbol{S}(t,2)]^{(2)} + 0.003\cdot[\boldsymbol{S}(t,2)]^{(3)} + 0.002\cdot[\boldsymbol{S}(t,2)]^{(4)} + 0.2\cdot[\boldsymbol{S}(t,2)]^{(5)} + 0.058\cdot[\boldsymbol{S}(t,2)]^{(6)} + 0.282\cdot[\boldsymbol{S}(t,2)]^{(7)},\ t \in \langle 0,\infty), \quad (48)$$

where the conditional coordinate safety functions

$$[\boldsymbol{S}(t,u)]^{(b)},\ t \in \langle 0,\infty),\ u = 1,2,\ b = 1, 2, \ldots,7,$$

are given in (Kołowrocki, 2020a; Kołowrocki & Magryta, 2020a).

The graph of this three-state port oil terminal critical infrastructure safety function, determined by (46)–(48), is shown in Figure 19.

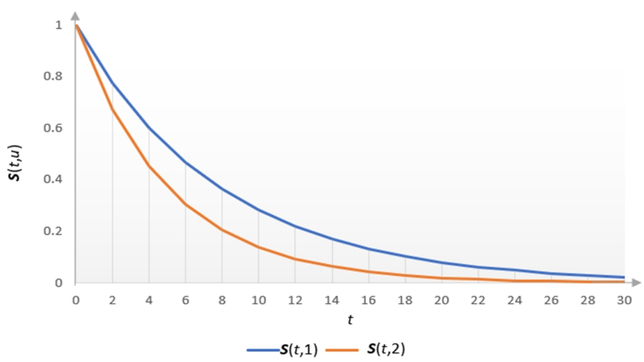

Figure 19. The graph of the port oil terminal critical infrastructure safety function coordinates.

The expected values and standard deviations of the terminal lifetimes in the safety state subsets

{1,2}, {2}, in years, determined according to (32)–(34), respectively are:

$$\boldsymbol{\mu}(1) \cong 7.89,\ \boldsymbol{\mu}(2) \cong 5.03, \quad (49)$$

$$\boldsymbol{\sigma}(1) \cong 7.91,\ \boldsymbol{\sigma}(2) \cong 5.03. \quad (50)$$

Considering (35) and (49), the terminal lifetimes in the safety state 1 and 2, in years, respectively are

$$\bar{\boldsymbol{\mu}}(1) \cong \boldsymbol{\mu}(1) - \boldsymbol{\mu}(2) = 2.86,$$
$$\bar{\boldsymbol{\mu}}(2) \cong \boldsymbol{\mu}(2) = 5.03. \quad (51)$$

Assuming that the critical safety state is $r = 1$ and applying (36), the system risk function is given by

$$\boldsymbol{r}(t) = 1 - \boldsymbol{S}(t,1),\ t \in \langle 0, \infty), \quad (52)$$

where $\boldsymbol{S}(t,1)$ is given by (47).
The graph of the port oil terminal risk function is presented in Figure 20.

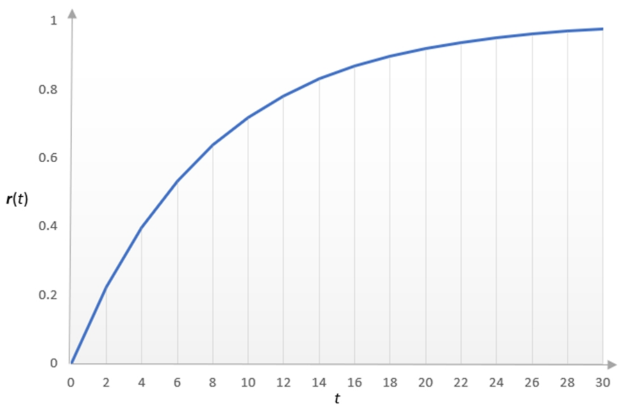

Figure 20. The graph of the port oil terminal risk function.

The moment t, when system risk function exceeds a permitted level d, $d \in (0,1)$, is

$$t \cong \boldsymbol{r}^{-1}(\delta) = 0.40 \text{ year}. \quad (53)$$

The port oil terminal critical infrastructure approximate mean intensities of ageing, determined according to (40) and (49), are:

$$\lambda(1) \cong 0.126743,\ \lambda(2) \cong 0.198807. \quad (54)$$

Hence, considering the values of the intensities of ageing of the port oil terminal without considering its operation process impact $\boldsymbol{\lambda}^0(1) = 0.115873$ and $\boldsymbol{\lambda}^0(2) = 0.18174$, determined in (Kołowrocki, 2020a), and applying (42), the coefficients of the operation process impact on the port oil terminal critical infrastructure intensities of ageing, are:

$$\boldsymbol{\rho}(1) \cong 1.09381,\ \boldsymbol{\rho}(2) \cong 1.09391. \quad (55)$$

Finally, the port oil terminal critical infrastructure resilience indicators, i.e. the coefficient of the port oil terminal critical infrastructure resilience to the operation process impact, by (44) and (55), are:

$$\boldsymbol{RI}(1) \cong 0.9142 = 91.42\%,$$
$$\boldsymbol{RI}(2) \cong 0.9142 = 91.42\%. \quad (56)$$

4.2. Safety of maritime ferry technical system impacted by its operation process

The considered maritime ferry is a passenger ship operating at the Baltic Sea between Gdynia and Karlskrona ports on regular everyday line (see: Figure 21).

Figure 21. The maritime ferry operating area.

The ferry technical system:

- S_1 – a navigational subsystem,
- S_2 – a propulsion and controlling subsystem,
- S_3 – a loading and unloading subsystem,
- S_4 – a stability control subsystem,
- S_5 – an anchoring and mooring subsystem.

The subsystems S_1, S_2, S_3, S_4, S_5, are forming a general series safety structure of the ferry technical system shown in Figure 22.

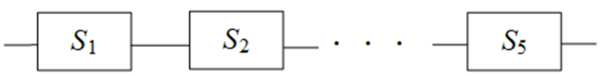

Figure 22. The general safety structure of ferry technical system safety.

Thus, taking into account the expert opinions concerned with the operation process of the considered ferry technical system, we distinguish the following as its eighteen operation states:

- an operation state z_1 – loading at Gdynia Port,
- an operation state z_2 – unmooring operations at Gdynia Port,
- an operation state z_3 – leaving Gdynia Port and navigation to *GD* buoy,
- an operation state z_4 – navigation at restricted waters from *GD* buoy to the end of *Traffic Separation Scheme*,
- an operation state z_5 – navigation at open waters from the end of *Traffic Separation Scheme* to *Angoering* buoy,
- an operation state z_6 – navigation at restricted waters from *Angoering* buoy to *Verko Berth* at Karlskrona,
- an operation state z_7 – mooring operations at Karlskrona Port,
- an operation state z_8 – unloading at Karlskrona Port,
- an operation state z_9 – loading at Karlskrona Port,
- an operation state z_{10} – unmooring operations at Karlskrona Port,
- an operation state z_{11} – ferry turning at Karlskrona Port,
- an operation state z_{12} – leaving Karlskrona Port and navigation at restricted waters to *Angoering* buoy,
- an operation state z_{13} – navigation at open waters from *Angoering* buoy to the entering Traffic Separation Scheme,
- an operation state z_{14} – navigation at restricted waters from the entering Traffic Separation Scheme to *GD* buoy,
- an operation state z_{15} – navigation from *GD* buoy to turning area,
- an operation state z_{16} – ferry turning at Gdynia Port,
- an operation state z_{17} – mooring operations at Gdynia Port,
- an operation state z_{18} – unloading at Gdynia Port.

The influence of the above defined operation states changing on the changes of the ferry technical system safety structure is as follows.

At the operation states z_1 and z_{18}, the ferry technical system is composed of two subsystems S_3 and S_4 forming a series structure shown in Figure 23.

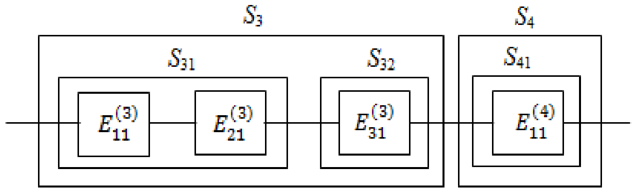

Figure 23. The scheme of the ferry technical system structure at the operation states z_1 and z_{18}.

At the operation states z_2, z_7, z_{10} and z_{17}, the ferry technical system is composed of three subsystems S_1, S_2 and S_5 forming a series structure shown in Figure 24.

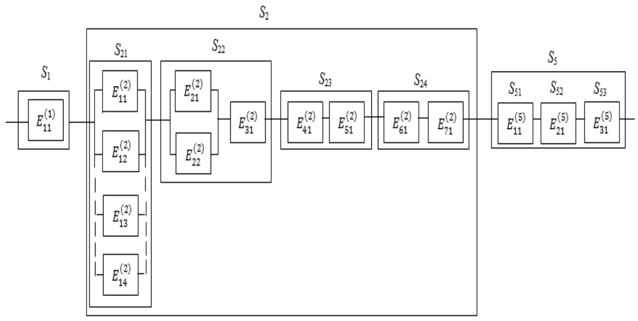

Figure 24. The scheme of the ferry technical system structure at the operation states z_2, z_7, z_{10} and z_{17}.

At the operation states z_3, z_{11}, z_{15} and z_{16}, the ferry technical system is composed of two subsystems S_1 and S_2 forming a series structure shown in Figure 25.

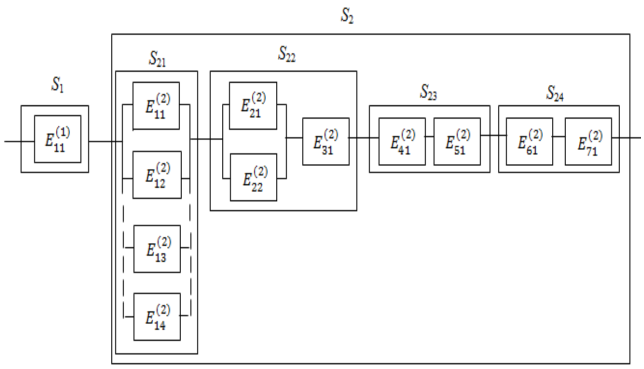

Figure 25. The scheme of the ferry technical system structure at the operation states z_3, z_{11}, z_{15} and z_{16}.

At the operation states z_4, z_5, z_{12}, z_{13} and z_{14}, the ferry technical system is composed of three subsystems S_1, S_2 and S_4 forming a series structure shown in Figure 26.

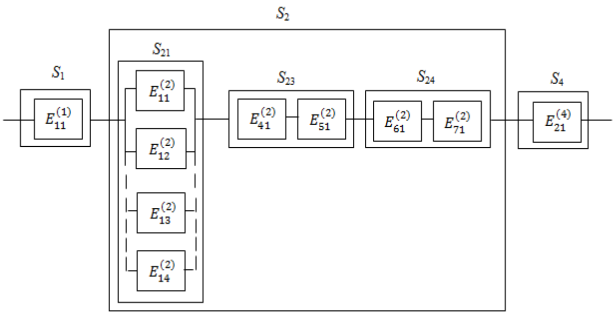

Figure 26. The scheme of the ferry technical system structure at the operation states z_4, z_5, z_{12}, z_{13} and z_{14}.

At the operation state z_6, the ferry technical system is composed of three subsystems S_1, S_2 and S_4 forming a series structure shown in Figure 27.

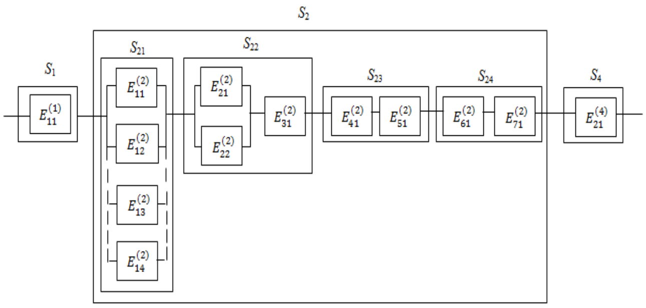

Figure 27. The scheme of the ferry technical system structure at the operation state z_6.

At the operation state z_8 and z_9, the ferry technical system is composed of two subsystems S_3 and S_4 forming a series structure shown in Figure 28.

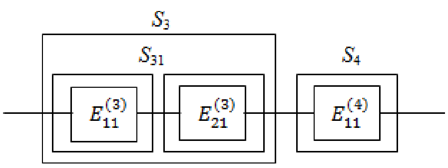

Figure 28. The scheme of the ferry technical system structure at the operation states z_8 and z_9.

To identify the unknown parameters of the ferry technical system operation process the suitable statistical data coming from its real realizations should be collected and on the basic of this data it is possible to estimate these parameters and to fix the port oil terminal characteristics. It is possible to collect these data because of the high frequency of the ferry voyages that result in a large number of its technical system operation process realizations. The ferry technical system operation process is very regular in the sense that the operation state changes are from the particular state z_b, $b = 1,2,\ldots,17$, to the neighboring state z_{b+1}, $b = 1,2,\ldots,17$, and from z_{18} to z_1 only.

The ferry technical system operation process $Z(t)$ main characteristics, the limit values of transient probabilities of at the particular operation states z_b, $b = 1,2,\ldots,18$, are (Kołowrocki, 2020a):

$$p_1 = 0.038,\ p_2 = 0.002,\ p_3 = 0.026,$$
$$p_4 = 0.036,\ p_5 = 0.363,\ p_6 = 0.026,$$
$$p_7 = 0.005,\ p_8 = 0.016,\ p_9 = 0.037,$$
$$p_{10} = 0.002,\ p_{11} = 0.003,\ p_{12} = 0.016,$$
$$p_{13} = 0.351,\ p_{14} = 0.034,\ p_{15} = 0.024,$$
$$p_{16} = 0.003,\ p_{17} = 0.005,\ p_{17} = 0.013. \quad (57)$$

We identify five safety states of the ferry technical system and its components:

- a safety state 4, the ferry operation is fully safe,
- a safety state 3, the ferry operation is less safe and more dangerous because of the possibility of environment pollution,
- a safety state 2, the ferry operation is less safe and more dangerous because of the possibility of environment pollution and causing small accidents,
- a safety state 1, the ferry operation is much less safe and much more dangerous because of the possibility of serious environment pollution and causing extensive accidents,
- a safety state 0, the ferry technical system is destroyed.

The maritime technical system safety function is given by the vector

$$\boldsymbol{S}(t,\cdot) = [\boldsymbol{S}(t,1), \boldsymbol{S}(t,2), \boldsymbol{S}(t,3), \boldsymbol{S}(t,4)], \quad (58)$$

$$t \in \langle 0, \infty),$$

with determined for $t \in \langle 0, \infty)$, according to (57) and (31), the coordinate safety functions:

$$\boldsymbol{S}(t,1) = 0.038 \cdot [\boldsymbol{S}(t,1)]^{(1)} + 0.002 \cdot [\boldsymbol{S}(t,1)]^{(2)}$$
$$+ 0.026 \cdot [\boldsymbol{S}(t,1)]^{(3)} + 0.036 \cdot [\boldsymbol{S}(t,1)]^{(4)}$$
$$+ 0.363 \cdot [\boldsymbol{S}(t,1)]^{(5)} + 0.026 \cdot [\boldsymbol{S}(t,1)]^{(6)}$$
$$+ 0.005 \cdot [\boldsymbol{S}(t,1)]^{(7)} + 0.016 \cdot [\boldsymbol{S}(t,1)]^{(8)}$$
$$+ 0.037 \cdot [\boldsymbol{S}(t,1)]^{(9)} + 0.002 \cdot [\boldsymbol{S}(t,1)]^{(10)}$$
$$+ 0.003 \cdot [\boldsymbol{S}(t,1)]^{(11)} + 0.016 \cdot [\boldsymbol{S}(t,1)]^{(12)}$$
$$+ 0.351 \cdot [\boldsymbol{S}(t,1)]^{(13)} + 0.034 \cdot [\boldsymbol{S}(t,1)]^{(14)}$$
$$+ 0.024 \cdot [\boldsymbol{S}(t,1)]^{(15)} + 0.003 \cdot [\boldsymbol{S}(t,1)]^{(16)}$$
$$+ 0.005 \cdot [\boldsymbol{S}(t,1)]^{(17)} + 0.013 \cdot [\boldsymbol{S}(t,1)]^{(18)}, \quad (59)$$

$\boldsymbol{S}(t,2) = 0.038\cdot[\boldsymbol{S}(t,2)]^{(1)} + 0.002\cdot[\boldsymbol{S}(t,2)]^{(2)}$
$+ 0.026\cdot[\boldsymbol{S}(t,2)]^{(3)} + 0.036\cdot[\boldsymbol{S}(t,2)]^{(4)}$
$+ 0.363\cdot[\boldsymbol{S}(t,2)]^{(5)} + 0.026\cdot[\boldsymbol{S}(t,2)]^{(6)}$
$+ 0.005\cdot[\boldsymbol{S}(t,2)]^{(7)} + 0.016\cdot[\boldsymbol{S}(t,2)]^{(8)}$
$+ 0.037\cdot[\boldsymbol{S}(t,2)]^{(9)} + 0.002\cdot[\boldsymbol{S}(t,2)]^{(10)}$
$+ 0.003\cdot[\boldsymbol{S}(t,2)]^{(11)} + 0.016\cdot[\boldsymbol{S}(t,3)]^{(12)}$
$+ 0.351\cdot[\boldsymbol{S}(t,2)]^{(13)} + 0.034\cdot[\boldsymbol{S}(t,2)]^{(14)}$
$+ 0.024\cdot[\boldsymbol{S}(t,2)]^{(15)} + 0.003\cdot[\boldsymbol{S}(t,2)]^{(16)}$
$+ 0.005\cdot[\boldsymbol{S}(t,2)]^{(17)} + 0.013\cdot[\boldsymbol{S}(t,2)]^{(18)},$ (60)

$\boldsymbol{S}(t,3) = 0.038\cdot[\boldsymbol{S}(t,3)]^{(1)} + 0.002\cdot[\boldsymbol{S}(t,3)]^{(2)}$
$+ 0.026\cdot[\boldsymbol{S}(t,3)]^{(3)} + 0.036\cdot[\boldsymbol{S}(t,3)]^{(4)}$
$+ 0.363\cdot[\boldsymbol{S}(t,3)]^{(5)} + 0.026\cdot[\boldsymbol{S}(t,3)]^{(6)}$
$+ 0.005\cdot[\boldsymbol{S}(t,3)]^{(7)} + 0.016\cdot[\boldsymbol{S}(t,3)]^{(8)}$
$+ 0.037\cdot[\boldsymbol{S}(t,3)]^{(9)} + 0.002\cdot[\boldsymbol{S}(t,3)]^{(10)}$
$+ 0.003\cdot[\boldsymbol{S}(t,3)]^{(11)} + 0.016\cdot[\boldsymbol{S}(t,3)]^{(12)}$
$+ 0.351\cdot[\boldsymbol{S}(t,3)]^{(13)} + 0.034\cdot[\boldsymbol{S}(t,3)]^{(14)}$
$+ 0.024\cdot[\boldsymbol{S}(t,3)]^{(15)} + 0.003\cdot[\boldsymbol{S}(t,3)]^{(16)}$
$+ 0.005\cdot[\boldsymbol{S}(t,3)]^{(17)} + 0.013\cdot[\boldsymbol{S}(t,3)]^{(18)},$ (61)

$\boldsymbol{S}(t,4) = 0.038\cdot[\boldsymbol{S}(t,4)]^{(1)} + 0.002\cdot[\boldsymbol{S}(t,4)]^{(2)}$
$+ 0.026\cdot[\boldsymbol{S}(t,4)]^{(3)} + 0.036\cdot[\boldsymbol{S}(t,4)]^{(4)}$
$+ 0.363\cdot[\boldsymbol{S}(t,4)]^{(5)} + 0.026\cdot[\boldsymbol{S}(t,4)]^{(6)}$
$+ 0.005\cdot[\boldsymbol{S}(t,4)]^{(7)} + 0.016\cdot[\boldsymbol{S}(t,4)]^{(8)}$
$+ 0.037\cdot[\boldsymbol{S}(t,4)]^{(9)} + 0.002\cdot[\boldsymbol{S}(t,4)]^{(10)}$
$+ 0.003\cdot[\boldsymbol{S}(t,4)]^{(11)} + 0.016\cdot[\boldsymbol{S}(t,4)]^{(12)}$
$+ 0.351\cdot[\boldsymbol{S}(t,4)]^{(13)} + 0.034\cdot[\boldsymbol{S}(t,4)]^{(14)}$
$+ 0.024\cdot[\boldsymbol{S}(t,4)]^{(15)} + 0.003\cdot[\boldsymbol{S}(t,4)]^{(16)}$
$+ 0.005\cdot[\boldsymbol{S}(t,4)]^{(17)} + 0.013\cdot[\boldsymbol{S}(t,4)]^{(18)},$ (62)

where the conditional coordinate safety functions

$[\boldsymbol{S}(t,u)]^{(b)},\ t \in \langle 0,\infty),$

$u = 1,2,3,4,\ b = 1,2,\ldots,18,$

are given in (Kołowrocki & Magryta, 2020c, 2021; Magryta-Mut, 2023b).
The graph of this five-state ferry technical system safety function is shown in Figure 29.
The expected values and standard deviations of the ferry technical system lifetimes in the safety state subsets {1,2,3,4}, {2,3,4}, {3,4}, {4} expressed in years respectively are:

$\boldsymbol{\mu}(1) \cong 1.694,\ \boldsymbol{\mu}(2) \cong 1.395,$
$\boldsymbol{\mu}(3) \cong 1.244,\ \boldsymbol{\mu}(4) \cong 1.114,$ (63)

$\boldsymbol{\sigma}(1) \cong 1.669,\ \boldsymbol{\sigma}(2) \cong 1.396,$
$\boldsymbol{\sigma}(3) \cong 1.230,\ \boldsymbol{\sigma}(4) \cong 1.102.$ (64)

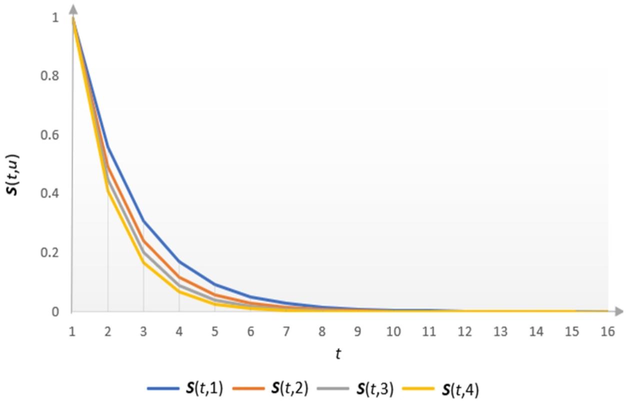

Figure 29. The graph of the ferry technical system safety function coordinates.

Considering (35) and (49), the terminal lifetimes in the safety state 1 and 2, in years, respectively are:

$\bar{\boldsymbol{\mu}}(1) \cong \boldsymbol{\mu}(1) - \boldsymbol{\mu}(2) = 0.299,$
$\bar{\boldsymbol{\mu}}(2) \cong \boldsymbol{\mu}(2) - \boldsymbol{\mu}(3) = 0.151,$
$\bar{\boldsymbol{\mu}}(3) \cong \boldsymbol{\mu}(3) - \boldsymbol{\mu}(4) = 0.130,$
$\bar{\boldsymbol{\mu}}(4) \cong \boldsymbol{\mu}(4) = 1.114.$ (65)

Since the critical safety state is r =1, then according to (36), the system risk function is given by

$\boldsymbol{r}(t) \cong 1 - \boldsymbol{S}(t,2)$ for $t \geq 0,$ (66)

where $\boldsymbol{S}(t,2)$ is given by (60).
The graph of the ferry technical system risk function is presented in Figure 30.

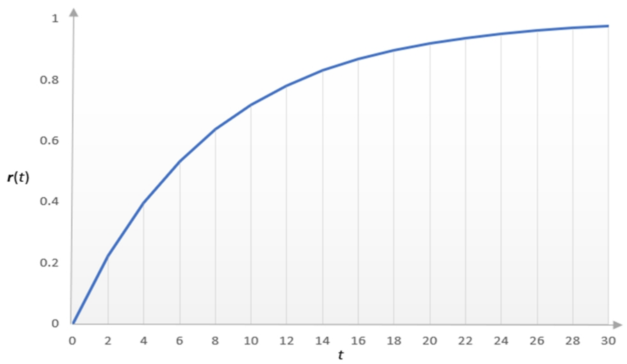

Figure 30. The graph of the ferry technical system risk function.

After applying (37) and (66), the moment t, when system risk function exceeds a permitted level d, $d \in (0,1)$, is

$t \cong \boldsymbol{r}^{-1}(\delta) = 0.073$ year. (67)

The ferry technical system approximate mean intensities of ageing, by applying (42) and considering (63), are:

$$\lambda(1) \cong 0.590363, \lambda(2) \cong 0.716869,$$
$$\lambda(3) \cong 0.803573, \lambda(4) \cong 0.897470. \quad (68)$$

The coefficients of the operation process impact on the ferry technical system intensities of ageing, are:

$$\boldsymbol{\rho}(1) \cong 1.044942, \boldsymbol{\rho}(2) \cong 1.058098,$$
$$\boldsymbol{\rho}(3) \cong 1.044645, \boldsymbol{\rho}(4) \cong 1.044655. \quad (69)$$

Finally, from (69), applying (42), the ferry technical system resilience indicators, i.e. the coefficients of the ferry technical system resilience to the operation process impact, are:

$$\boldsymbol{RI}(1) \cong 0.9570 = 95.70\%,$$
$$\boldsymbol{RI}(2) \cong 0.9451 = 94.51\%,$$
$$\boldsymbol{RI}(3) \cong 0.9573 = 95.73\%,$$
$$\boldsymbol{RI}(4) \cong 0.9573 = 95.73\%. \quad (70)$$

5. Conclusion

The general safety analytical model of complex multistate technical system related to its operation process was presented. The procedure based on this system safety model was practically applied to the port oil terminal critical infrastructure and the maritime ferry technical system safety examination. This procedure can be used in safety evaluation of various real complex technical systems and critical infrastructures (Gouldby et al., 2010; Kołowrocki & Magryta, 2020c; Lauge et al., 2015; Magryta, 2020) and together with the linear programming (Klabjan & Adelman, 2016) to their safety and operation cost optimization (Kołowrocki, 2021; Kołowrocki & Magryta, 2020a, 2020b, 2022; Magryta-Mut, 2020, 2023a, 2023b; Ramirez-Marqueza & Coid, 2007).

Further research can be related to considering other impacts on the system safety and its operation cost, for instance a very important impact related to climate-weather factors (Kołowrocki, 2021, 2022a, 2022b; Kołowrocki & Kuligowska, 2018) and resolving the issues of critical infrastructure (Lauge et al., 2015) safety and operation cost optimization and discovering optimal values of safety, operation cost and resilience indicators of system impacted by the operation and climate-weather conditions (Kołowrocki, 2021). These developments can also benefit the mitigation of critical infrastructure accident consequences (Bogalecka, 2020) and inside and outside dependences (De Porcellinis et al., 2009; Holden et al., 2013; Kołowrocki, 2021, 2022a, 2022b; Nieuwenhuijs et al., 2008; Ouyang, 2014; Rinaldi et al., 2001; Svedsen & Wolthunsen, 2007) and to minimize the system operation cost and to improve critical infrastructure resilience to operation and climate-weather conditions (Kołowrocki, 2021, 2022a, 2022b).

The proposed developments of optimization procedures and perspective of future research applied to system operation cost and to safety and resilience optimization of the complex systems and critical infrastructures can give practically important possibility of these systems effectiveness improvement through the proposing their new operation strategy application and their components safety and operation cost optimization (Magryta-Mut, 2023a, 2023b).

As a consequence of the presented results and suggested their developments, the further research could be focused on safety analysis of multistate ageing complex systems and critical infrastructure networks, considering their ageing, inside dependencies, outside impacts, including separate and joint operation and climate-weather change impacts and the use of the achieved new results to improve their safety, strengthen their resilience and minimizing and mitigate the effects of their degradation and failures (Kołowrocki, 2022b).

Acknowledgment

The paper presents the results developed in the research work granted by Polish Safety and Reliability Association.

References

Ancione, G., Paltrinieri, N. & Milazzo, M.F. 2020. Integrating real-time monitoring data in risk assessment for crane related offshore operations. *Journal of Marine Science and Engineering* 8(7), 1–28, 532.

Bautista, B.L., Torres, C.I. & Landesa, P.L. 2020. A condition-based maintenance for complex systems consisting of two different types of components. K. Kołowrocki et al. (Eds.), *Safety and Reliability of Systems and Processes,* *Summer Safety and Reliability Seminar* 2020. Gdynia Maritime University, Gdynia, 7–16.

Berg, H.P. & Petrek, N. 2018. Threats and possible approaches of vulnerability of natural hazards on road infrastructure. *Journal of Polish Safety and Reliability Association Summer Safety and Reliability Seminars* 9(3), 1–10.

Bogalecka, M. 2020. *Consequences of Maritime Critical Infrastructure Accidents. Environmental Impacts. Modeling – Identification – Prediction – Optimization – Mitigation*. Elsevier, Amsterdam – Oxford – Cambridge.

Brunelle, R.D. & Kapur, K.C. 1999. Review and classification of reliability measures for multistate and continuum models. *IEEE Transactions* 31, 1117–1180.

Čepin, M. 2020. The extended living probabilistic safety assessment. *Proceedings of the Institution of Mechanical Engineers. Part. O, Journal of Risk and Reliabilit*y 234(1), 183–192.

Dąbrowska, E. 2020. Safety analysis of car wheel system impacted by operation process. *Safety and Reliability of Systems and Processes, Summer Safety and Reliability Seminar* 5, 61–75.

De Porcellinis, S., Oliva, G., Panzieri, S. & Setola, R. 2009. A holistic-reductionistic approach for modeling interdependencies. *Critical Infrastructure Protection III*. Springer, 215–227.

Ferreira, F. & Pacheco, A. 2007. Comparison of level-crossing times for Markov and semi-Markov processes. *Statistics & Probability Letters* 77(2), 151–157.

Glynn, P.W. & Haas, P.J. 2006. Laws of large numbers and functional central limit theorems for generalized semi-Markov processes. *Stochastic Models* 22(2), 201–231.

Gouldby, B.P., Schultz, M.T., Simm, J.D. & Wibowo, J.L. 2010. Beyond the Factor of Safety: Developing Fragility Curves to Characterize System Reliability, *Report in Water Resources Infrastructure Program ERDC SR-10-1*, Prepared for Headquarters. U.S. Army Corps of Engineers, Washington.

Grabski, F. 2015. *Semi-Markov Processes: Application in System Reliability and Maintenance*. Elsevier, Amsterdam – Boston – Heidelberd – London – New York – Oxford – Paris – San Diego – San Francisco – Sydney – Tokyo.

Holden, R., Val, D.V., Burkhard, R. & Nodwell, S. 2013. A network flow model for interdependent infrastructures at the local scale. *Safety Science* 53(3), 51–60.

Klabjan, D. & Adelman, D. 2016. Existence of optimal policies for semi-Markov decision processes using duality for infinite linear programming. *Society for Industrial and Applied Mathematics Control and Optimization* 44(6), 2104–212.

Kołowrocki, K. 2000. On asymptotic approach to multi-state systems reliability evaluation. *Recent Advances in Reliability Theory: Methodology, Practice and Inference.* Birkhauser, Boston 11, 163–180.

Kołowrocki, K. 2003. Asymptotic approach to reliability analysis of large systems with degrading components. *International Journal of Reliability, Quality and Safety Engineering* 10(3), 249–288.

Kołowrocki, K. 2005. *Reliability of Large Systems*. Elsevier, Amsterdam – Boston – Heidelberg – London – New York – Oxford – Paris – San Diego – San Francisco – Singapore – Sydney – Tokyo.

Kołowrocki, K. 2008. Reliability and risk analysis of multi-state systems with degrading components. *International Journal of Reliability, Quality and Safety Engineering* 6(2), 213–228.

Kołowrocki, K. 2011. Reliability modelling of complex systems. H. Pham (Eds.), *Safety and Risk Modelling and Its Applications*. Springer, 3–54.

Kołowrocki, K. 2014. *Reliability of Large and Complex Systems. 2nd Edition.* Elsevier, Amsterdam – Boston –Heidelberg – London – New York – Oxford – Paris – San Diego – San Francisco – Singapore – Sydney – Tokyo.

Kołowrocki, K. 2020a. Port Oil Terminal Safety Examination. *Scientific Journals of the Maritime University of Szczecin* 61(133), 143–151.

Kołowrocki, K. 2020b. Safety analysis of multistate ageing car wheel system with dependent components. K. Kołowrocki et al. (Eds.), *Safety and Reliability of Systems and Processes, Summer Safety and Reliability Seminar*, 101–116.

Kołowrocki, K. 2021. Safety analysis of critical infrastructure impacted by operation and climate-weather changes – theoretical backgrounds, K. Kołowrocki et al. (Eds.), *Safety and Reliability of Systems and Processes, Summer Safety and Reliability Seminar*, 139–180.

Kołowrocki, K. 2022a. Safety analysis of multistate ageing system with inside dependences and outside impacts. *Current Research in Mathematical and Computer Sciences III*. A. Lecko

(Ed.). University of Warmia and Mazury Press, 175–214.

Kołowrocki, K. 2022b. European Union Global Critical Infrastructure Safety Management System – research project proposition. K. Kołowrocki et al. (Eds.), *Safety and Reliability of Systems and Processes, Summer Safety and Reliability Seminar*, 79–92.

Kołowrocki, K. & Kuligowska, E. 2018. Operation and climate-weather change impact on maritime ferry safety. *Safety and Reliability – Safe Societies in a Changing World*. Taylor and Francis, 849–854.

Kołowrocki, K. & Magryta, B. 2020a. Port oil terminal reliability optimization. *Scientific Journals Maritime University of Szczecin.*

Kołowrocki, K. & Magryta, B. 2020b. Changing system operation states influence on its total operation cost. *DepCoS-RELCOMEX 2020: Theory and Applications of Dependable Computer Systems*, 355–365.

Kołowrocki, K. & Magryta-Mut, B. 2020c. Safety of maritime ferry technical system impacted by operation process, K. Kołowrocki et al. (Eds.), *Safety and Reliability of Systems and Processes, Summer Safety and Reliability Seminar*, 117–134.

Kołowrocki, K. & Magryta-Mut, B. 2022. Operation cost and safety optimization of maritime transportation system. *Current Research in Mathematical and Computer Sciences III*. A. Lecko (Ed.). University of Warmia and Mazury Press, 215–247.

Kołowrocki, K. & Magryta-Mut, B. 2023. Safety and operation cost optimization of complex multistate ageing systems. *Advances in Reliability and Maintainability Methods and Engineering Applications: Essays in Honor of Professor Hong-Zhong Huang on his 60th Birthday*, Springer.

Kosmowski, K.T. 2021. Functional Safety and Cybersecurity Analysis and Management in Smart Manufacturing Systems, K.B. Misra (Ed.) *Handbook of Advanced Performability Engineering*, Springer Nature Switzerland AG, 3.

Kossow, A. & Preuss, W. 1995. Reliability of linear consecutively-connected systems with multistate components. *IEEE Transactions on Reliability* 44, 518–522.

Kvassay, M., Rusnak, P., Zaitseva, E. & Kostolny, J. 2020. Minimal cut vectors of multi-state systems identified using logic differential calculus and multi-valued decision diagrams, *30th European Safety and Reliability Conference, ESREL 2020 and 15th Probabilistic Safety Assessment and Management Conference, PSAM* 2020, 3053–3060.

Lauge, A., Hernantes, J. & Sarriegi, J.M. 2015. Critical infrastructure dependencies: a holistic, dynamic and quantitative approach. *International Journal of Critical Infrastructure Protection* 8, 16–23.

Li, W. & Pham, H. 2005. Reliability modeling of multi-state degraded systems with multi-competing failures and random shocks. *IEEE Transactions on Reliability* 54(2), 297–303.

Limnios, N. & Oprisan, G. 2005. *Semi-Markov Processes and Reliability*. Birkhauser. Boston.

Magryta, B. 2020. Reliability approach to resilience of critical infrastructure impacted by operation process. *Journal of KONBiN* 50(1), 131–153.

Magryta-Mut, B. 2020. Safety optimization of maritime ferry technical system, K. Kołowrocki et al. (Eds.), *Safety and Reliability of Systems and Processes, Summer Safety and Reliability Seminar*, 175–182.

Magryta-Mut, B. 2023a. Port oil terminal operation cost optimization, K. Kołowrocki et al. (Eds.), *Safety and Reliability of Systems and Processes, Summer Safety and Reliability Seminar*, abc–def.

Magryta-Mut, B. 2023b. *Safety and operation cost optimization of port and maritime transportation systems*, PhD Thesis (under completion).

Mercier, S. 2008. Numerical bounds for semi-Markovian quantities and application to reliability. *Methodology and Computing in Applied Probability* 10(2), 179–198.

Natvig, B. 2007. Multi-state reliability theory. *Encyclopedia of Statistics in Quality and Reliability*. Wiley, New York, 1160–1164.

Nieuwenhuijs, A., Luiijf, E. & Klaver, M. 2008. Modeling dependencies in critical infrastructures. *Critical Infrastructure Protection II, IFIP International Federation for Information Processing*, Springer, Boston, Massachusetts 253, 205–213.

Ouyang, M. 2014. Review on modelling and simulation of interdependent critical infrastructure systems. *Reliability Engineering & System Safety* 121, 43–60.

Ramirez-Marqueza, J.E. & Coit, D.W. 2007. Multi-state component criticality analysis for reliability improvement in multi-state systems. *Reliability Engineering & System Safety* 92, 1608–1619.

Rinaldi, S., Peerenboom, J. & Kelly, T. 2001. Identifying, understanding and analyzing critical infrastructure interdependencies, *IEEE Control Systems Magazine* 21(6), 11–25.

Svedsen, N. & Wolthunsen, S. 2007. Connectivity models of interdependency in mixed-type critical infrastructure networks. *Information Security Technical Report* 12(1), 44–55.

Szymkowiak, M. 2018a. Characterizations of distributions through aging intensity, *IEEE Transactions on Reliability* 67.

Szymkowiak, M. 2018b. Generalized aging intensity functions. *Reliability Engineering and System Safety* 178.

Szymkowiak, M. 2019. Lifetime Analysis by Aging Intensity Functions. *Studies in Systems, Decision and Control*. Springer International Publishing 196.

Tang, H., Yin, B.Q. & Xi, H.S. 2007. Error bounds of optimization algorithms for semi-Markov decision processes. *International Journal of Systems Science* 38(9).

Wang, Z., Huang, H.Z., Li, Y. & Xiao, N.C. 2011. An approach to reliability assessment under degradation and shock process. Reliability, *IEEE Transactions on Reliability* 60(4), 852–863.

Xue, J. 1985. On multi-state system analysis. *IEEE Transactions on Reliability* 34, 329–337.

Xue, J. & Yang, K. 1995a. Dynamic reliability analysis of coherent multi-state systems. *IEEE Transactions on Reliability* 4(44), 683–688.

Xue, J. & Yang, K. 1995b. Symmetric relations in multi-state systems. *IEEE Transactions on Reliability* 4(44), 689–693.

Yingkui, G. & Jing, L. 2012. Multi-state system reliability: a new and systematic review. *Procedia Engineering* 29, 531–536.

Zaitseva, E. & Levashenko, V. 2017. Reliability analysis of multi-state system and multiple-valued logic, *International Journal of Quality & Reliability Management* 34(6), 862–878.